J Mol Model (2013) 19:2549–2557
DOI 10.1007/s00894-013-1805-0

ORIGINAL PAPER

# Natural bond orbital, nuclear magnetic resonance analysis and hybrid-density functional theory study of σ-aromaticity in $Al_2F_6$, $Al_2Cl_6$, $Al_2Br_6$ and $Al_2I_6$

**Davood Nori-Shargh · Hooriye Yahyaei · Seiedeh Negar Mousavi · Akram Maasoomi · Hakan Kayi**

Received: 21 January 2013 / Accepted: 11 February 2013 / Published online: 2 March 2013


**Abstract** Natural bond orbital (NBO), nuclear magnetic resonance (NMR) analysis and hybrid-density functional theory based method (B3LYP/Def2-TZVPP) were used to investigate the correlation between the nucleus-independent chemical shifts [NICS, as an aromaticity criterion], $\sigma_{Al(1)\text{-}X2(b)} \rightarrow \sigma^*_{Al(3)\text{-}X4(b)}$ electron delocalizations and the dissociation energies of $Al_2F_6$, $Al_2Cl_6$, $Al_2Br_6$ and $Al_2I_6$ to $2AlX_3$ (X=F, Cl, Br, I). The results obtained showed that the dissociation energies of $Al_2F_6$, $Al_2Cl_6$, $Al_2Br_6$ and $Al_2I_6$ decrease from $Al_2F_6$ to $Al_2I_6$. Like aromatic molecules, these compounds have relatively significant negative $NICS_{iso}(0)$ values. Clearly, based on magnetic criteria, they exhibit aromatic character and make it possible to consider them as σ-delocalized aromatic species, such as Möbius σ-aromatic species. The σ-aromatic character which is demonstrated by their $NICS_{iso}(0)$ values decreases from $Al_2F_6$ to $Al_2I_6$. The $NICS_{iso}$ values are dominated by the in-plane $\sigma_{22}$ (i.e., $\sigma_{yy}$, the plane containing halogen atoms bridged) chemical shift components. The increase of the $NICS_{iso}$ values explains significantly the decrease of the corresponding dissociation energies of $Al_2F_6$, $Al_2Cl_6$, $Al_2Br_6$ and $Al_2I_6$. Importantly, the NBO results suggest that in these compounds the dissociation energies are controlled by the stabilization energies associated with $\sigma_{Al(1)\text{-}X2(b)} \rightarrow \sigma^*_{Al(3)\text{-}X4(b)}$ electron delocalizations. The decrease of the stabilization energies associated with $\sigma_{Al(1)\text{-}X2(b)} \rightarrow \sigma^*_{Al(3)\text{-}X4(b)}$ electron delocalizations is in accordance with the variation of the calculated $NICS_{iso}$ values. The correlations between the dissociation energies of $Al_2F_6$, $Al_2Cl_6$, $Al_2Br_6$ and $Al_2I_6$, $\sigma_{Al(1)\text{-}X2(b)} \rightarrow \sigma^*_{Al(3)\text{-}X4(b)}$ electron delocalizations, natural atomic orbitals (NAOs) and $NICS_{iso}$ values have been investigated.

**Keywords** Hybrid-DFT calculations · $Al_2F_6$ · $Al_2Cl_6$ · $Al_2Br_6$ · $Al_2I_6$ · AM1* · NBO · NICS

D. Nori-Shargh (✉) · S. N. Mousavi · A. Maasoomi
Department of Chemistry, Arak Branch,
Islamic Azad University, Arak, Iran
e-mail: nori_ir@yahoo.com

H. Yahyaei
Department of Chemistry, Zanjan Branch,
Islamic Azad University, Zanjan, Iran

H. Kayi
Institute for Theoretical Chemistry,
Department of Chemistry and Biochemistry,
The University of Texas,
Austin, TX 78712, USA

H. Kayi
Department of Chemical Engineering and Applied Chemistry,
Atilim University,
Ankara 06836, Turkey

## Introduction

Aluminum chloride ($AlCl_3$) (as the main compound of aluminium and chlorine) can be found in three different phases (i.e., solid, liquid, gas phases) which depends on the temperature. The Al centers exhibit octahedral coordination geometry in the solid $AlCl_3$ [1]. Contrary to the boron halides, the aluminum halides are dimers in the gas phase. $Al_2Cl_6$ dimers are found in the vapor and liquid phases. The $Al_2Cl_6$ dimers dissociate into trigonal planar $AlCl_3$ at higher temperatures. Unlike more ionic halides such as sodium chloride, the melt of $Al_2Cl_6$ poorly conducts electricity [2]. The tendency to dimerization increases by the reduction of the *p*-orbital tendency to participate in π bonding in period 3 as compared with period 2 of the periodic table of the elements. Each Al atom acts as an acid toward a Cl atom bonded to the other Al

atom, therefore, $Al_2Cl_6$ is a self acid–base complex [3]. $Al_2Cl_6$ is widely used as a Lewis acid catalyst in organic reactions (e.g., Friedel-Crafts alkylation and acylation) [3, 4].

In 1999, Aarset and co-workers [5] used gas-phase electron-diffraction (GED) data together with results from ab initio molecular orbital and normal coordinate calculations to determine the structures of the aluminum trihalides $AlX_3$ (X=Cl, Br, I) and the chloride and bromide dimers ($Al_2Cl_6$ and $Al_2Br_6$). The results of these authors indicated that the $X_{bridged}$-Al-$X_{bridged}$ bond angles increase from $Al_2Cl_6$ to $Al_2Br_6$.

Although there is insufficient published experimental and theoretical data about the structures of $AlX_3$ and $Al_2X_6$ (X= Cl, Br, I) [5–8], there is no published experimental or quantitative theoretical data about the donor-acceptor delocalization effects and the aromaticity on the structural properties of $Al_2X_6$ (X=F, Cl, Br, I) (see Scheme 1).

The $\sigma$-aromaticity, associated with $\sigma \rightarrow \sigma^*$ electron delocalization causes lowering of ring strain energies for the saturated rings [9–12]. This evidence for $\sigma$-aromaticity is further supported by theoretical strain energy (TSE) [10]. According to ab initio valence bond (VB) computations at the VBSCF/cc-PVTZ level, the $\sigma$-aromatic stabilization energy of cyclopropane is, at most, 3.5 kcal$mol^{-1}$ relative to propane [11].

In this study, we used a natural bond orbital (NBO) [13, 14] interpretation and hybrid-density functional theory based method to explain the impact of the stabilization energies associated with donor-acceptor electron delocalizations and aromaticity [15–23] on the structural parameters of $Al_2F_6$, $Al_2Cl_6$, $Al_2Br_6$ and $Al_2I_6$ and their dissociation energies to $2AlX_3$ (X=F, Cl, Br, I). The quantitative relationship between the aromatic character [15] of the four atom membered rings of $Al_2F_6$, $Al_2Cl_6$, $Al_2Br_6$ and $Al_2I_6$ [with $4N$ electrons] associated with $\sigma \rightarrow \sigma^*$ hyperconjugations and dissociation energies is demonstrated by their nucleus-independent-chemical-shift (NICS) values [15–22].

It should be noted that many systems in organic chemistry consist of monocyclic arrays of orbitals in which there is one or an odd number of overlaps between adjacent orbitals of different sign. These molecules do not have a closed shell with $4N+2$ electrons but rather need $4N$ electrons for stability and with $4N+2$ electrons they are antiaromatic. These molecular species have been termed Möbius because the molecular orbital situation is quite like that of Heilbronner's Möbius cyclic polyenes [23, 24].

Importantly, if the Möbius array of necessity contains at least one plus-minus overlap in its basis set, this system might be more stable than a Hückel one, while the Hückel cycle does not. Although a plus-minus overlap represents a local anti-bonding and energy raising contribution, Möbius molecular orbitals have the property of having their molecular orbital coefficients very small near the site of plus-minus overlap. This fact can be particularly justified by the lower energy Möbius atomic orbitals [24].

## Computational details

Hybrid-density functional theory calculations [25–29] were performed using the B3LYP method [26, 27] and the Def2-TZVPP basis set [30] with the PC GAMESS program suite [31] for optimizing the geometries of $Al_2F_6$, $Al_2Cl_6$, $Al_2Br_6$ and $Al_2I_6$. We also performed AM1* semiempirical calculations using the VAMP 10.0 program to optimize the structures of above dimers [32]. Energy minimum molecular geometries were located by minimizing energy, with respect to all geometrical coordinates without imposing any symmetry constraints. The nature of the stationary points for $Al_2F_6$, $Al_2Cl_6$, $Al_2Br_6$, $Al_2I_6$ and $AlX_3$ (X=F, Cl, Br, I) has been determined by means of the number of imaginary frequencies. For the minimum state structure, only the real frequency values were accepted, and in the transition-state structure, only a single imaginary frequency value was accepted [33, 34].

An NBO analysis was then performed for for $Al_2F_6$, $Al_2Cl_6$, $Al_2Br_6$ and $Al_2I_6$ by the NBO 5.G program contained in the PC-GAMESS interface [15]. In the NBO analysis the electronic wavefunctions are interpreted in terms of a set of occupied Lewis and a set of unoccupied non-Lewis localized orbitals. The delocalization effects (or donor–acceptor charge transfers) can be estimated from the presence of off-diagonal elements of the Fock matrix in the NBO basis. The NBO program searches for an optimal natural Lewis structure, which has the maximum occupancy of its occupied NBOs, and in general agrees with the pattern of bonds and lone pairs of the standard structural Lewis formula. Therefore, the new orbitals are more stable than pure Lewis orbitals, stabilizing the wave function and giving a set of molecular orbitals equivalent to canonical molecular orbitals.

The bonding and antibonding orbital occupancies, energies, the stabilization energies associated with

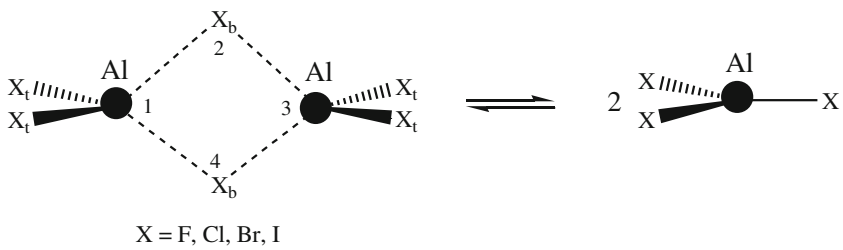


X = F, Cl, Br, I

**Scheme 1** Schematic representation of the equilibrium between the $Al_2X_6$ dimers and $AlX_3$ monomers

$\sigma_{Al(1)\text{-}X2(b)} \rightarrow \sigma^*_{Al(3)\text{-}X4(b)}$ electron delocalizations and corresponding off-diagonal elements ($F_{ij}$) were calculated (see Fig. 1).

The resonance energy associated with donor-acceptor electron delocalization is proportional to $S^2/\Delta E$ where $S$ is the orbital integral of the two interacting orbitals and $\Delta E$ is the energy difference between the donor and acceptor orbitals [13]. In addition, the resonance (stabilization) energy ($E_2$) associated with $i \rightarrow j$ delocalization is explicitly estimated by following equation:

$$E_2 = q_i \frac{F^2(i,j)}{\varepsilon_j - \varepsilon_i}, \quad (1)$$

where $q_i$ is the ith donor orbital occupancy, $\varepsilon_i$, $\varepsilon_j$, are diagonal elements (orbital energies) and $F$(i,j) off-diagonal elements, respectively, associated with the NBO Fock matrix. In the NBO method, the donor-acceptor electron interactions can be studied separately because this method allows separation of the energy contribution due to donor-acceptor electronic interactions from those caused by steric and electrostatic interactions. Therefore the NBO approach permits consideration of charge delocalization. It has to be noted that the NBO analysis is a sufficient approach to investigate the stereoelectronic interactions on the structures, dynamic behaviors and reactivity of chemical compounds [35].

Also, we used the GIAO-B3LYP/Def2-TZVPP method in order to calculate the nucleus-independent chemical shift (NICS) values. The experimental values of the NMR chemical shifts are vibrational average, whereas the computational results correspond to a fixed geometry at 0 K. It should be remembered that the NMR chemical shifts are not too sensitive to the optimized geometry [36].

## Results and discussion

### Dissociation energies

The values of the thermodynamic functions $H$, $S$, $G$ and the $\Delta G$, $\Delta S$ and $\Delta H$ parameters at 25 °C and 1 atm pressure for $Al_2F_6$, $Al_2Cl_6$, $Al_2Br_6$, $Al_2I_6$ and $AlX_3$ (X= F, Cl, Br, I) as calculated at the B3LYP/Def2-TZVPP level of theory, are given in Table 1. The absolute values of the thermodynamic properties certainly cannot be calculated at the accuracy level shown in this table; however, the quantities of interest here are the relative values of the thermodynamic functions for different conformations of the same molecule. We expect that the errors in such differences will be very small and the corresponding errors between the different closely related compounds will be minimal. The smooth variation among the calculated values supports this expectation.

Based on the B3LYP/Def2-TZVPP results, the calculated Gibbs free energy difference values between $Al_2F_6$, $Al_2Cl_6$, $Al_2Br_6$, $Al_2I_6$ and $2AlX_3$ (X=F, Cl, Br, I) (i.e., $\Delta G_{2AlX3\text{-}Al2X6}$) decrease from $Al_2F_6$ to $Al_2I_6$ (see Table 1 and Fig. 1). The corresponding $\Delta G_{2AlX3\text{-}Al2X6}$ values are 38.19, 14.53, 9.49 and 7.18 kcal mol$^{-1}$, respectively, as calculated at the B3LYP/Def2-TZVPP level of theory. Based on the results obtained, the dissociation energies with regared to $Al_2X_6 \rightarrow 2AlX_3$ reactions decrese from $Al_2F_6$ to $Al_2I_6$ which shows the easiness of Al-X-Al 3-center-2-electron bond breaking from fluorine to iodine derivatives. Although this fact seems to be expectable, we want to caliry if there are correlations between the easiness of the breaking of Al-X-Al 3-center-2-electron bonds, Möbius σ-aromatic character (one the basic concepts in chemistry) in $Al_2F_6$, $Al_2Cl_6$, $Al_2Br_6$ and $Al_2I_6$ associated

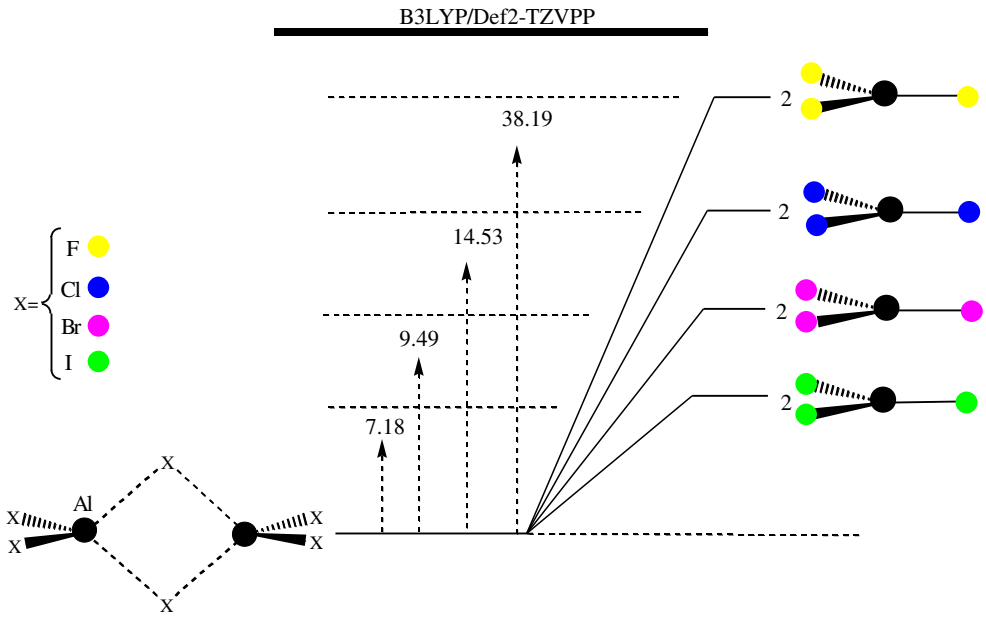


**Fig. 1** B3LYP/Def2-TZVPP calculated potential energy surfaces ($\Delta G^a$: in kcal mol$^{-1}$) for the dissociations of $Al_2F_6$, $Al_2Cl_6$, $Al_2Br_6$, $Al_2I_6$ to $2AlX_3$ (X=F, Cl, Br, I)

**Table 1** B3LYP/Def2-TZVPP calculated thermodynamic functions ($H$, $G$, $S$) and parameters [$\Delta H$, $\Delta G$ (in hartree) and $\Delta S$ (in $cal\,mol^{-1}\,K^{-1}$)] at 25 °C and 1 atm pressure for $Al_2F_6$, $Al_2Cl_6$, $Al_2Br_6$, $Al_2I_6$ and $AlX_3$ (X=F, Cl, Br, I)

| Geometries | H | S | G | ΔH[a] | ΔS[a] | ΔG[a] |
|---|---|---|---|---|---|---|
| $Al_2F_6$ | −1084.760541 | 96.914 | −1084.806588 | 0.000000 (0.00)[b] | 0.000000 | 0.000000 (0.00)[b] |
| 2 $AlF_3$ | −1084.692517 | 111.978 | −1084.745722 | (0.068024) (42.69)[b] | 15.064 | 0.060866 (38.19)[b] |
| $Al_2Cl_6$ | −3246.728963 | 114.653 | −3246.783438 | 0.000000 (0.00)[b] | 0.000000 | 0.000000 (0.00)[b] |
| 2 $AlCl_3$ | −3246.694537 | 138.370 | −3246.760281 | (0.03) (21.60)[b] | 23.717 | (0.02) (14.53)[b] |
| $Al_2Br_6$ | −15930.436429 | 132.377 | −15930.49932 | 0.000000 (0.00)[b] | 0.000000 | 0.000000 (0.00)[b] |
| 2 $AlBr_3$ | −15930.409213 | 157.827 | −15930.48420 | 0.027216 (17.08)[b] | 25.45 | 0.01512 (9.49)[b] |
| $Al_2I_6$ | −2272.100313 | 143.905 | −2272.168687 | 0.000000 (0.00)[b] | 0.000000 | 0.000000 (0.00)[b] |
| 2 $AlI_3$ | −2272.082694 | 144.290 | −2272.151251 | 0.017619 (11.06)[b] | 0.385 | 0.011436 (7.18)[b] |

[a]Relative to the corresponding dimers

[b]Numbers in parenthesis are in $kcal\,mol^{-1}$

with $\sigma_{Al(1)\text{-}X2(b)} \rightarrow \sigma^*_{Al(3)\text{-}X4(b)}$ electron delocalizations, orbital energies and off-diagonal elements, bond orders, structural parameters and natural hybrid orbitals (NHOs).

## NICS values

The nucleus-independent-chemical-shift (NICS) values for the four-membered rings of $Al_2F_6$, $Al_2Cl_6$, $Al_2Br_6$ and $Al_2I_6$ arise from the same mechanism. The calculated NICS values can be used to compare the aromaticity for the same types of molecules.

The GIAO-B3LYP/Def2-TZVPP calculated $NICS_{iso}$ values at the approximate centers of the four-membered rings of $Al_2F_6$, $Al_2Cl_6$, $Al_2Br_6$ and $Al_2I_6$, $NICS_{iso}(0)$, are −7.0, −4.9, −4.3 and −3.5 ppm, respectively (the $NICS_{iso}$ values are reported as the negative of the actual size. The variation of the $NICS_{iso}(0.0)$ values (by considering their actual sizes) are in the same trend with the variation of the in-plane $\sigma_{22}$ (i.e., $\sigma_{yy}$, the plane containing halogen atoms bridged) values. Therefore, the $NICS_{iso}(0.0)$ values of $Al_2F_6$, $Al_2Cl_6$, $Al_2Br_6$ and $Al_2I_6$ are controlled and dominated by in-plane $\sigma_{22}$ chemical shift components (see Table 2). The in-plane $\sigma_{22}$ chemical shift (with their actual size) components at the approximate centers of the four-membered rings of $Al_2F_6$, $Al_2Cl_6$, $Al_2Br_6$ and $Al_2I_6$ are found to be −15.5773, −17.9633, −21.1429 and −23.8768 ppm, respectively.

The $NICS_{iso}(0.2)$, $NICS_{iso}(0.4)$, $NICS_{iso}(0.6)$ and $NICS_{iso}(0.8)$ values are obtained above the plane on a line passing through the point where NICS(0.0) values were evaluated (see Table 2 and Fig. 2). Based on the results obtained, the calculated $NICS_{iso}$ values of $Al_2F_6$, $Al_2Cl_6$,

**Table 2** GIAO-B3LYP/Def2-TZVPP calculated absolute chemical shifts, $\sigma_{iso}$, and chemical shift tensor components ($\sigma_{11}$, $\sigma_{22}$ and $\sigma_{33}$, in ppm) for $Al_2F_6$, $Al_2Cl_6$, $Al_2Br_6$ and $Al_2I_6$

| | $NICS_{iso}(0.0)$ | | | |
|---|---|---|---|---|
| Compound | $Al_2F_6$ | $Al_2Cl_6$ | $Al_2Br_6$ | $Al_2I_6$ |
| $\sigma_{iso}$ | −7.0117 | −4.8597 | −4.3428 | −3.4931 |
| $\sigma_{11}$ | 21.1750 | 16.5380 | 15.9799 | 15.8543 |
| $\sigma_{22}$ | −15.5773 | −17.9633 | −21.1429 | −23.8768 |
| $\sigma_{33}$ | 15.4374 | 16.0045 | 18.1913 | 18.5018 |
| | NICS(0.2) | | | |
| $\sigma_{iso}$ | −6.6567 | −4.6347 | −4.1323 | −3.3251 |
| $\sigma_{11}$ | 19.5142 | 15.7147 | 15.2401 | 15.1912 |
| $\sigma_{22}$ | −13.8474 | −17.0209 | −20.1919 | −22.9515 |
| $\sigma_{33}$ | 14.3035 | 15.2104 | 17.3488 | 17.7355 |
| | NICS(0.4) | | | |
| $\sigma_{iso}$ | −5.6434 | −4.0264 | −3.5848 | −2.8485 |
| $\sigma_{11}$ | 15.2294 | 13.3656 | 13.1793 | 13.3668 |
| $\sigma_{22}$ | −9.6372 | −14.2282 | −17.4233 | −20.4462 |
| $\sigma_{33}$ | 11.3379 | 12.9419 | 14.9985 | 15.6249 |
| | NICS(0.6) | | | |
| $\sigma_{iso}$ | −4.2749 | −3.1546 | −2.7961 | −2.2065 |
| $\sigma_{11}$ | 10.0184 | 10.2403 | 10.3722 | 10.8032 |
| $\sigma_{22}$ | −4.9122 | −10.7033 | −13.7697 | −16.8247 |
| $\sigma_{33}$ | 7.7184 | 9.9269 | 11.7857 | 12.6409 |
| | NICS(0.8) | | | |
| $\sigma_{iso}$ | −2.9122 | −2.2561 | −1.9730 | −0.3888 |
| $\sigma_{11}$ | 5.3987 | 7.0230 | 7.4168 | 8.0309 |
| $\sigma_{22}$ | −1.2018 | −7.0825 | −9.8784 | −12.9480 |
| $\sigma_{33}$ | 4.5398 | 6.8276 | 8.3804 | −1.4906 |

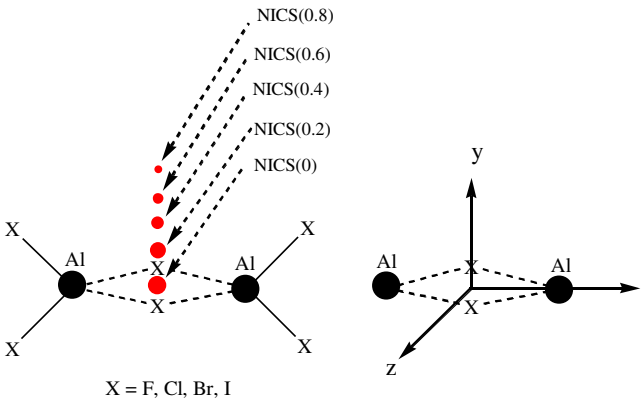


**Fig. 2** Schematic representation of the $NICS_{iso}(0)$ values at the approximate centers of $Al_2F_6$, $Al_2Cl_6$, $Al_2Br_6$, $Al_2I_6$ and the $NICS_{iso}(0.2)$, $NICS_{iso}(0.4)$, $NICS_{iso}(0.6)$, $NICS_{iso}(0.8)$ values obtained above the plane on a line passing through the point where $NICS_{iso}(0)$ values were evaluated

$Al_2Br_6$ and $Al_2I_6$ increase from NICS(0.0) to the corresponding NICS(0.8). The in-plane $\sigma_{22}$ chemical shift components at the approximate centers of the four-membered rings decrease from the four-membered rings of $Al_2F_6$ to $Al_2I_6$. This trend is observed for the calculated values of the in-plane $\sigma_{22}$ chemical shift components of $NICS_{iso}(0.2)$, $NICS_{iso}(0.4)$, $NICS_{iso}(0.6)$ and $NICS_{iso}(0.8)$ (see Table 2). The decrease of the in-plane $\sigma_{22}$ chemical shift components of $NICS_{iso}(0.2)$, $NICS_{iso}(0.4)$ and $NICS_{iso}(0.6)$ is in excellent agreement with the decrease of the calculated $\Delta G_{2AlX3\text{-}Al2X6}$ values of the dissociation processes from $Al_2F_6$ to $Al_2I_6$ (see Tables 1 and 2).

The results indicate that with the increase of $NICS_{iso}(0)$ values from $Al_2F_6$ to $Al_2I_6$, the corresponding $\Delta G_{2AlX3\text{-}Al2X6}$ values of the dissociation processes decrease from $Al_2F_6$ to $Al_2I_6$. The plot of $\Delta G_{2AlX3\text{-}Al2X6}$ versus $NICS_{iso}(0)$ values, shown in Fig. 3, reveals a linear relationship between

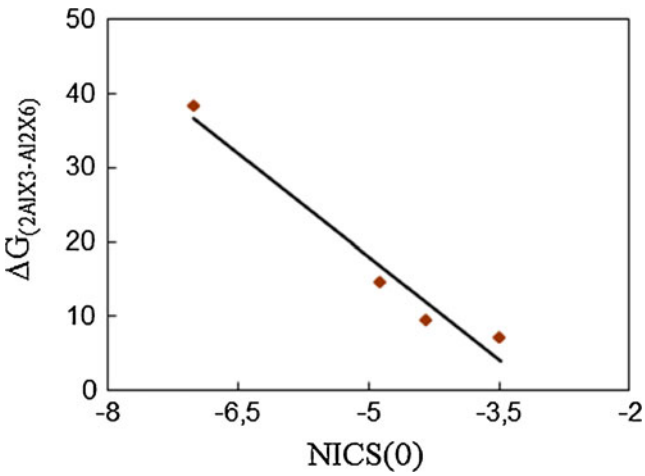


**Fig. 3** Calculated dissociation energy values for $Al_2F_6$, $Al_2Cl_6$, $Al_2Br_6$ and $Al_2I_6$, $\Delta G_{2AlX3\text{-}Al2X6}$, plotted as a function of NICS(0) [$\Delta G_{2AlX3\text{-}Al2X6}$=−28.57–9.32 [NICS(0)], $R^2$=0.96]

them. Consequently, the calculated $\Delta G_{2AlX3\text{-}Al2X6}$ values could be proposed as a criterion for the evaluation of the Möbius σ-aromatic character in $Al_2F_6$, $Al_2Cl_6$, $Al_2Br_6$ and $Al_2I_6$.

## Stabilization energies ($E_2$) associated with the electron delocalizations

The NBO analysis shows that $Al_2F_6$, $Al_2Cl_6$, $Al_2Br_6$ and $Al_2I_6$ dimers benefit from stabilizations associated with the donor-acceptor electron delocalizations. Based on the optimized ground state geometries using the B3LYP/Def2-TZVPP method, the NBO analysis of donor-acceptor (bond-antibond) interactions showed that the stabilization energies associated with $\sigma_{Al(1)\text{-}X2(b)} \rightarrow \sigma^*_{Al(3)\text{-}X4(b)}$ electron delocalizations decrease from $Al_2F_6$ to $Al_2I_6$ (see Table 3 and Scheme 2). This trend is in agreement with the variation of the dissociation processes of $Al_2F_6$, $Al_2Cl_6$, $Al_2Br_6$ and $Al_2I_6$ dimers to their corresponding monomers.

The plot of stabilization energies ($E_2$) associated with $\sigma_{Al(1)\text{-}X2(b)} \rightarrow \sigma^*_{Al(3)\text{-}X4(b)}$ electron delocalizations versus $NICS_{iso}(0)$ values, shown in Fig. 4, reveals a linear relationship between them. Importantly, the decrease of the $\sigma_{Al(1)\text{-}X2(b)} \rightarrow \sigma^*_{Al(3)\text{-}X4(b)}$ electron delocalizations demonstrates the decrease of the σ-aromatic character of the corresponding four-membered ring from $Al_2F_6$ to $Al_2I_6$.

## Orbital energies and off-diagonal elements

The energy differences between donor ($\sigma_{Al(1)\text{-}X2(b)}$) and acceptor ($\sigma^*_{Al(3)\text{-}X4(b)}$) orbitals [i.e., $\Delta(E\sigma^*_{Al(3)\text{-}X4(b)} - E\sigma_{Al(1)\text{-}X2(b)})$] for $Al_2F_6$, $Al_2Cl_6$, $Al_2Br_6$ and $Al_2I_6$ are 1.17, 0.73, 0.66 and 0.54 a.u., respectively, as calculated by NBO analysis. It can be expected that the strong acceptor antibonding orbital ($\sigma^*_{Al(3)\text{-}X4(b)}$) of $Al_2I_6$ (compared to those in $Al_2Br_6$, $Al_2Cl_6$ and $Al_2F_6$) may give rise to strong $\sigma_{Al(1)\text{-}X2(b)} \rightarrow \sigma^*_{Al(3)\text{-}X4(b)}$ electron delocalization (see Table 3). It should be noted that the decrease of the *orbital overlap* ($S$) [off-diagonal elements ($F_{ij}$)] values for the $\sigma_{Al(1)\text{-}X2(b)} \rightarrow \sigma^*_{Al(3)\text{-}X4(b)}$ electron delocalization from $Al_2F_6$ to $Al_2I_6$ could reduce the corresponding stabilization energies (see Table 3). Since the second order perturbation energy ($E_2$) is related to the $F_{ij}$ and $\Delta(E_{acceptor} - E_{donor})$ values, it seems that in $Al_2F_6$, $Al_2Cl_6$, $Al_2Br_6$ and $Al_2I_6$ the $F_{ij}$ could affect and control the order of the stabilization energies ($E_2$) associated with the corresponding $\sigma_{Al(1)\text{-}X2(b)} \rightarrow \sigma^*_{Al(3)\text{-}X4(b)}$ electron delocalizations.

## Bond orders

The $\sigma_{Al(1)\text{-}X2(b)} \rightarrow \sigma^*_{Al(3)\text{-}X4(b)}$ electron delocalizations can be correlated to structural effects through the bond orders

**Table 3** NBO calculated stabilization energies ($E_2$), off-diagonal elements ($F_{ij}$), orbital energies and orbital occupancies, natural hybridized orbitals (NHOs) and polarization coefficient ($a$) based on the calculated geometries using B3LYP/Def2-TZVPP level of theory, for for $Al_2F_6$, $Al_2Cl_6$, $Al_2Br_6$ and $Al_2I_6$ dimer

| $E_2$ (kcal mol$^{-1}$) | $Al_2F_6$ | $Al_2Cl_6$ | $Al_2Br_6$ | $Al_2I_6$ |
|---|---|---|---|---|
| $(\sigma_{Al1\text{-}X2(bridged)} \rightarrow \sigma^*_{Al3\text{-}X4(bridged)}) \times 4$ | 9.4 | 8.6 | 8.1 | 7.1 |
| Orbital energy (a.u.) | | | | |
| $E\sigma_{Al1\text{-}X2(bridged)}$ | −0.88 | −0.65 | −0.63 | −0.54 |
| $E\sigma^*_{Al3\text{-}X4(bridged)}$ | 0.29 | 0.08 | 0.03 | 0.00 |
| $\Delta(E\sigma^*_{Al3\text{-}X4(bridged)} - E\sigma_{Al1\text{-}X2(bridged)})$ | 1.17 | 0.73 | 0.66 | 0.54 |
| $F_{ij}$ (a.u.) | | | | |
| $\sigma_{Al1\text{-}X2(bridged)} \rightarrow \sigma^*_{Al3\text{-}X4(bridged)}$ | 0.048 | 0.036 | 0.032 | 0.023 |
| Orbital hybridization | | | | |
| $X(Al\text{-}X_{bridged})$ | $sp^{2.53}$ | $sp^{3.52}$ | $sp^{3.96}$ | $sp^{4.68}$ |
| Bond order (Wiberg Bond Index) | | | | |
| $\sigma_{Al1\text{-}X2(bridged)}$ | 0.26 | 0.45 | 0.50 | 0.58 |
| Bond order (Atom-Atom Overlap-Weighted NAO Bond Orders) | | | | |
| $\sigma_{Al1\text{-}X2(bridged)}$ | 0.35 | 0.55 | 0.58 | 0.64 |
| NHO | | | | |
| $h_{Al1}$ | $sp^{3.89}d^{0.20}$ | $sp^{3.83}d^{0.14}$ | $sp^{3.87}d^{0.11}$ | $sp^{3.96}d^{0.08}$ |
| $h_{X2}$ | $Sp^{2.53}d^{0.00}$ | $Sp^{3.52}d^{0.02}$ | $Sp^{3.95}d^{0.02}$ | $Sp^{4.68}d^{0.03}$ |
| a | | | | |
| $a_{Al1}$ | 0.2397 | 0.3485 | 0.3773 | 0.4286 |
| $a_{X2}$ | 0.9709 | 0.9373 | 0.9261 | 0.9035 |

**Scheme 2** Schematic representation of the electron delocalization between bonding and anti-bonding orbitals in $Al_2F_6$, $Al_2Cl_6$, $Al_2Br_6$ and $Al_2I_6$

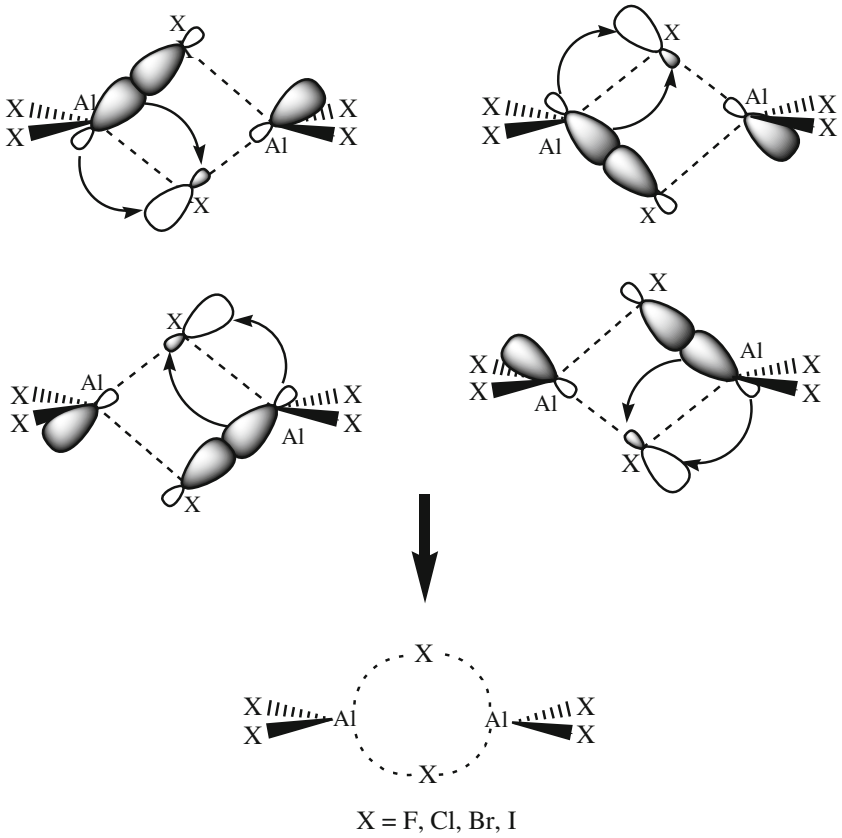

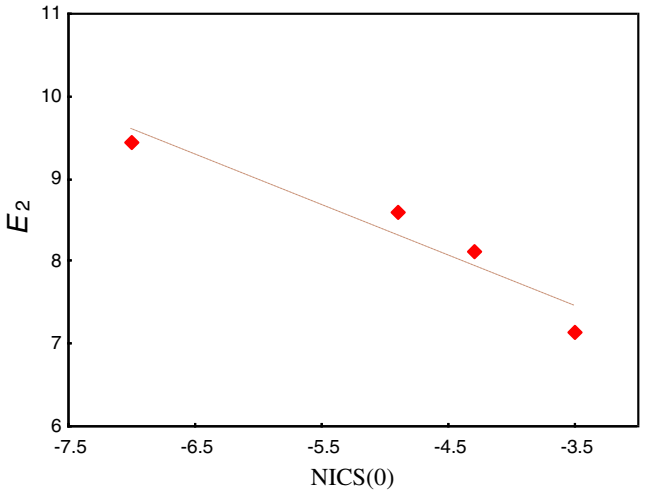


**Fig. 4** Calculated stabilization energy values associated with σAl1-*X*2(bridged)→σAl3-X4(bridged) electron delocalization in $Al_2F_6$, $Al_2Cl_6$, $Al_2Br_6$ and $Al_2I_6$, $E_2$, potted as a function of NICSiso(0) [[$E_2$=5.3132–0.6113 [NICSiso(0)], $R_2$=0.91] $R^2$=0.91]

[e.g., Wiberg bond index, *WBI*: the sum of squares of off-diagonal density matrix elements between atoms), as formulated in terms of the natural atomic orbital (NAO) basis set and atom-atom overlap-weighted NAO bond orders (AAOWNAOBO)]. The calculated bond orders (*WBI* and AAOWNAOBO] for $Al_1$-$X_2$ (bridged) bonds increase from $Al_2F_6$ to $Al_2I_6$ (see Table 3). Importantly, the increase of the calculated *WBI* and AAOWNAOBO values for $\sigma_{Al1X2(bridged)}$ bonds can be explained by the decrease of the $\sigma_{Al(1)\text{-}X2(b)} \rightarrow \sigma^*_{Al(3)\text{-}X4(b)}$ electron delocalizations from $Al_2F_6$ to $Al_2I_6$.

## Structural parameters and natural hybrid orbitals (NHOs)

Representative structural parameters for $Al_2F_6$, $Al_2Cl_6$, $Al_2Br_6$, $Al_2I_6$ and $AlX_3$ (X=F, Cl, Br, I) obtained from the B3LYP/Def2-TZVPP level and also semiempirical AM1* calculations are shown in Fig. 5. Although results from most of the semiempirical methods, which may include AM1* as well, could be less reliable for some specific types of problems compared with the DFT methods, the comparison of the results from one of the most modern semiempirical techniques AM1* and B3LYP/Def2-TZVPP calculations in this study can provide a clear picture to reparameterize some of the AM1* parameters.

As expected for aromatic systems, all dimers studied in this work have planar and quasi-square structure, due to the delocalization of the σ-electrons. In analogy to benzene, in which aromaticity is responsible for its perfect hexagonal structure with all equal C-C bonds, rather than the classical alternating single and double bonds, [37] $Al_2F_6$, $Al_2Cl_6$, $Al_2Br_6$ and $Al_2I_6$ have equal Al-$X_b$ bonds (see Fig. 5).

It should be noted that the aluminum-halogen bond lengths in AM1* are found around 0.1-0.2 Å shorter compared with the B3LYP and the experimental results. These deviations in the bond lengths originate from the systematical errors of chlorine parameterization in the AM1*, and also from the large errors obtained for the aluminum-halogen geometrical parameters that were previously reported in the original AM1* parameterization studies [38–40].

Interestingly, studies of structural parameters show that the $\theta_{Al\text{-}Xb\text{-}Al}$ bond angles decreases from $Al_2F_6$ to $Al_2I_6$. This fact can be explained by the increase of the *p*-orbital character from the hybridized orbital of the bridged halogen atom from $Al_2F_6$ to $Al_2I_6$ (see Table 3).

To gain more insight into the structural and bonding properties of the dimers studied in this work, the natural atomic orbitals (NAOs) were also quantitatively analyzed. The NAOs are centered on a particular atom. According to the simple bond orbital picture, a NBO is defined as an orbital formed from natural hybridized orbitals (NHOs). Therefore, the NBO for a localized $\sigma_{Al1\text{-}F2}$ bond is defined as:

$$\sigma_{Al1-X2} = a_{Al1}h_{Al1} + a_{X2}h_{X2}, \quad (2)$$

where $h_{Al1}$ and $h_{X2}$ are the natural hybrids centered on atoms $Al_1$ and $X_2$. Also $a_{Al1}$ and $a_{X2}$ are their corresponding polarization coefficient. NBOs closely correspond to the picture of localized bonds and lone pairs as basic units of molecular structure. Therefore, ab initio wavefunctions can be conveniently interpreted in terms of the classical Lewis structure concepts by transforming these functions to NBO form.

The resulted natural atomic orbitals *h* on $Al_1$ and $X_2$ with their corresponding polarization coefficient *a* values are given in Table 3. The results obtained show that the *d* character of the $Al_1$ NHO in the $\sigma_{Al1\text{-}X2}$ bond orbital decreases on going from $Al_2F_6$ to $Al_2I_6$ but the *p* character of the $X_2$ NHO increases. This fact can explain the decrease of the $\theta_{Al\text{-}Xb\text{-}Al}$ bond angles from $Al_2F_6$ to $Al_2I_6$ (see Fig. 5 and Table 3).

The resulted polarization coefficient *a* values of the $Al_1$ atoms for the $\sigma_{Al1\text{-}X2}$ bond orbitals increase from $Al_2F_6$ to $Al_2I_6$ while the corresponding values for the $X_2$ atoms decrease (see Table 3). The difference is given by a "Δ" parameter, $\Delta(a_{Al1}- a_{X2})$. The calculated $\Delta(a_{Al1}- a_{X2})$ values for $Al_2F_6$, $Al_2Cl_6$, $Al_2Br_6$ and $Al_2I_6$ are 0.7312, 0.5888, 0.5488 and 0.4749, respectively. Based on the results obtained, the ionic character of the $\sigma_{Al1\text{-}X2}$ bond decreases from $Al_2F_6$ to $Al_2I_6$. This fact is in accordance with the decrease of the electronegative character on going from fluorine to chlorine which justifies the increase of the $\sigma_{Al1\text{-}X2}$ bond orbital energies and also

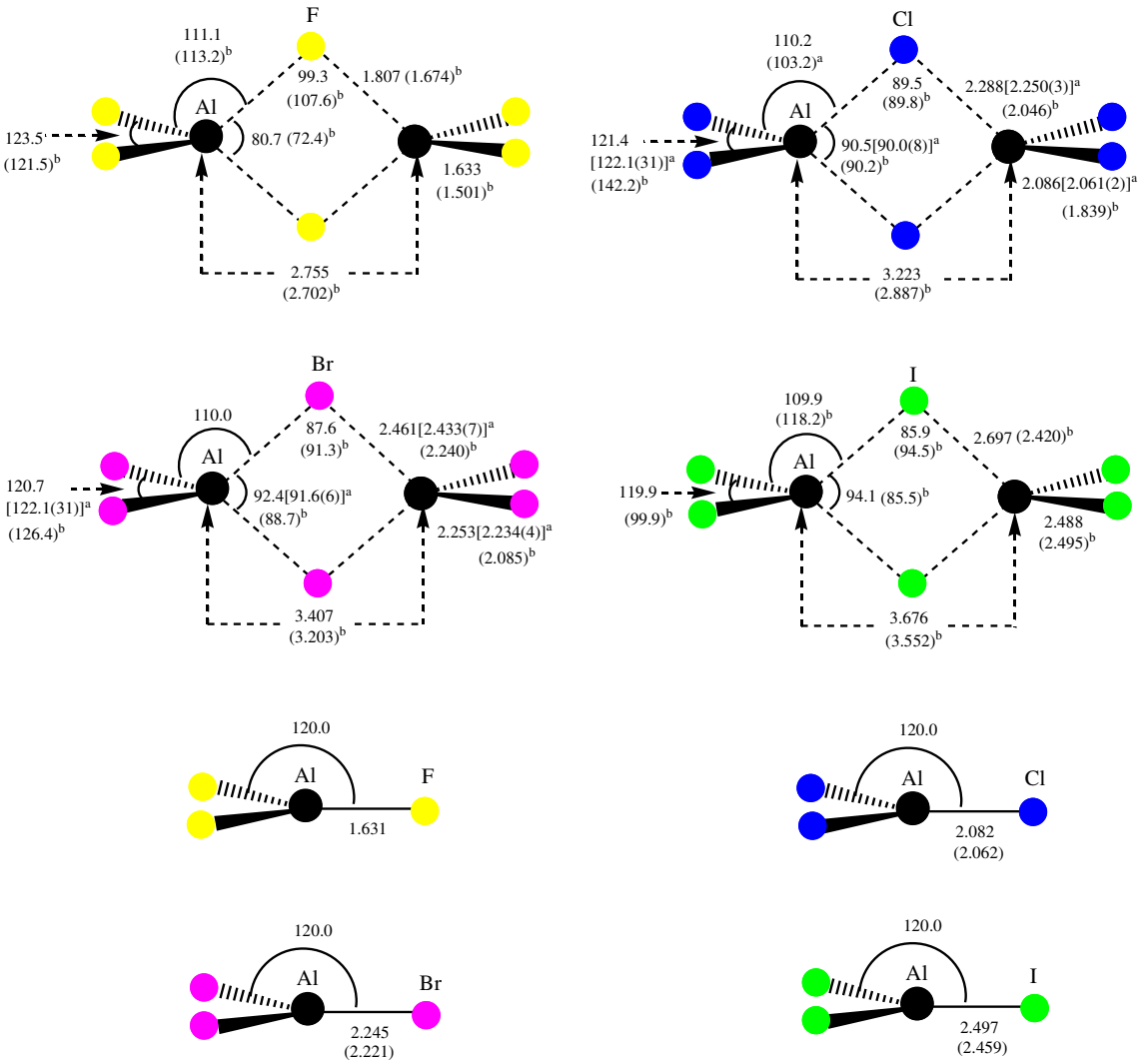


**Fig. 5** B3LYP/Def2-TZVPP calculated structural parameters of $Al_2F_6$, $Al_2Cl_6$, $Al_2Br_6$, $Al_2I_6$ and $AlX_3$ (X=F, Cl, Br, I). The calculated bond length and bond angle values are in angstrom (Å) and degree (º), respectively. a)From the combined gas-phase electron-diffraction (GED)/ab initio study [see ref. 5]. b)From AM1* calculations [see refs. 38–40]

the decrease of the $\sigma^*_{Al1\text{-}X2}$ anti-bond orbital energies from $Al_2F_6$ to $Al_2I_6$ (see Table 3).

## Conclusions

The NBO, NMR analysis and hybrid-density functional theory based method provided a useful picture from bonding point of view for $Al_2F_6$, $Al_2Cl_6$, $Al_2Br_6$, $Al_2I_6$ and $AlX_3$ (X=F, Cl, Br, I). The calculated $\Delta G_{2AlX3\text{-}Al2X6}$ values between $Al_2F_6$, $Al_2Cl_6$, $Al_2Br_6$, $Al_2I_6$ and $2AlX_3$ (X=F, Cl, Br, I) decrease from $Al_2F_6$ to $Al_2I_6$.

The Möbius $\sigma$-aromatic character decreases from $Al_2F_6$ to $Al_2I_6$. The decrease of Möbius σ-aromatic character (the increase of the $NICS_{iso}$ values) explains significantly the decrease of the corresponding dissociation energies of $Al_2F_6$, $Al_2Cl_6$, $Al_2Br_6$ and $Al_2I_6$ to $2AlX_3$ (X=F, Cl, Br, I). Importantly, the NBO results suggest that in these compounds the dissociation energies are controlled by the stabilization energies associated with $\sigma_{Al(1)\text{-}X2(b)} \rightarrow \sigma^*_{Al(3)\text{-}X4(b)}$ electron delocalizations and the decrease of this electron delocalization facilitates the dissociation processes. The decrease of the $\sigma_{Al(1)\text{-}X2(b)} \rightarrow \sigma^*_{Al(3)\text{-}X4(b)}$ electron delocalizations justifies the variation of the corresponding $NICS_{iso}$ values. This concept can be generalized to the other systems in the chemical problem investigations.

**Acknowledgments** This research has been supported by Islamic Azad University, Arak Branch. Some parts of this work have been supported by Welch Foundation at the University of Texas at Austin, Grant No. F-100.

## References


1. Wells F (1984) Structural inorganic chemistry. Clarendon, Oxford
2. Greenwood NN, Earnshaw A (1984) Chemistry of the elements. Pergamon, Oxford
3. Shriver DF, Atkins PW, Langford CH (1992) Inorganic chemistry. Oxford University Press, Oxford
4. Olah GA, Meyer MW (1963) In: Friedelcrafts and related reactions. Olah GA (Ed.), Interscience,New york 1: 623 765
5. Aarset K, Shen Q, Thomassen H, Richardson AD, Hedberg K (1999) Molecular structure of the aluminum halides, $Al_2Cl_6$, $AlCl_3$, $Al_2Br_6$, $AlBr_3$, and $AlI_3$, obtained by gas-phase electron-diffraction and ab initio molecular orbital calculations. J Phys Chem A 103:1644–1652. doi:10.1021/jp9842042, and references therein
6. Curtiss LA (1978) Molecular orbital studies of Al2F6 and Al2Cl6 using a minimal basis set. Int J Quantum Chem 14:709–715. doi:10.1002/qua.560140602
7. Williams SD, Harper W, Mamantov G, Tortorelli LJ, Shankle G (1996) Ab initio MO study of selected aluminum and boron chlorides and fluorides: Comparison with $^{11}B$ NMR spectra of a tetrachloroborate melt. J Comput Chem 17:1696–1711. doi:10.1002/(SICI)1096-987X(19961130)
8. Scholz G, Schöffel K, Jensen VR, Bache Ø, Ystenesc M (1994) Vibrational frequencies of AlF3: An ab initio MO study evaluating different methods on a tricky case. Chem Phys Lett 230:196–202. doi:10.1016/0009-2614(94)01101-X
9. Göller A, Clark T (2000) σ*-aromaticity in three membered rings. J Mol Model 6:133–149. doi:10.1007/PL00010724
10. Li ZH, Moran D, Fan KN, PvR S (2005) Sigma-aromaticity and sigma-antiaromaticity in saturated inorganic rings. J Phys Chem A 109:3711–3716. doi:10.1021/jp048541o
11. Wu W, Ma B, Wu JIC, PvR S, Mo Y (2009) Is cyclopropane really the sigma-aromatic paradigm? CHEM EUR J 15:9730–9736. doi:10.1002/chem.200900586
12. Havenith RWA, De Proft F, Fowler PW, Geerlings P (2005) sigma-Aromaticity in H-3(+) and Li-3(+): insights from ring-current maps. Chemical Physics Letters 407:391–396. doi:10.1016/j.cplett.2005.03.099
13. Glendening ED, Badenhoop JK, Reed AE, Carpenter JE, Bohmann JA, Morales CM, Weinhold F (2004) NBO Version 5.G. Theoretical Chemistry Institute. University of Wisconsin, Madison
14. Reed AE, Curtiss LA, Weinhold F (1988) Intermolecular interactions from a natural bond orbital, donor-acceptor viewpoint. Chem Rev 88:899–926. doi:10.1021/cr00088a005
15. Chen Z, Wannere CS, Corminboeuf C, Puchta R, PvR S (2005) Nucleus-independent chemical shifts (NICS) as an aromaticity criterion. Chem Rev 105:3842–3888. doi:10.1021/cr030088+
16. Garratt PG (1986) Aromaticity. Wiley, New York
17. Katritzky A, Barczynski P, Musumarra G, Pisano D, Szafran M (1989) Aromaticity as a quantitative concept. 1. A statistical demonstration of the orthogonality of classical and magnetic aromaticity in five- and six-membered heterocycles. J Am Chem Soc 111:7–15. doi:10.1021/ja00183a002
18. Jug K, Köster AM (1991) Aromaticity as a multi-dimentional phenomenon. J Phys Org Chem 4:163–169. doi:10.1002/poc.610040307
19. Minkin VI, Glukhovstsev MN, Simkin BY (1994) Aromaticity and Antiaromaticity. Wiley, New York
20. Schleyer PR, Jiao H (1996) What is Aromaticity? Pure & Appl Chem 68:209–218. doi:10.1351/pac199668020209
21. von Ragué Schleyer P, Maerker C, Dransfeld A, Jiao H, van Eikema Hommes NJR (1996) Nucleus-independent chemical shifts: a simple and efficient aromaticity probe. J Am Chem Soc 118:6317–6318. doi:10.1021/ja960582d
22. Nyulaszi L, PvR S (1999) Hyperconjugative-aromaticity: how to make cyclopentadiene aromatic. J Am Chem Soc 121:6872–6875. doi:10.1021/ja983113f
23. Heilbronner E (1964) Tetrahedron Lett 5(29):1923–1928
24. Zimmerman HE (1971) Acc Chem Res 4:272–228
25. Becke AD (1993) Density-functional thermochemistry. III. The role of exact exchange. J Chem Phys 98:5648–5652. doi:10.1063/1.464913
26. Yang LW, Parr RG (1988) Development of the Colle-Salvetti conelation energy formula into a functional of the electron density. Phys Rev B 37:785–789. doi:10.1103/PhysRevB.37.785
27. Vosko SH, Wilk L, Nusair M (1980) Accurate spin-dependent electron liquid correlation energies for local spin density calculations: a critical analysis. Can J Phys 58:1200–1211. doi:10.1139/p80-159
28. Stephens PJ, Devlin FJ, Chabalowski CF, Frisch MJ (1994) Ab initio calculation of vibrational absorption and circular dichroism spectra using density functional force fields. J Phys Chem 98:11623–11627. doi:10.1021/j100096a001
29. Seminario JM, Politzer P (1995) An introduction to density functional theory in chemistry. In: Seminario JM (ed) Density functional theory: a tool for chemistry. Elsevier, Amsterdam
30. Weigend F, Ahlrichs R (2005) Balanced basis sets of split valence, triple zeta valence and quadruple zeta valence quality for H to Rn: design an assessment of accuracy. Phys Chem Chem Phys 7:3297–3305. doi:10.1039/B508541A
31. Schmidt MW, Baldridge KK, Boatz JA, Elbert ST, Gordon MS, Jensen JH, Koseki S, Matsunaga N, Nguyen KA, Su SJ, Windus TL, Dupuis M, Montgomery JA (1993) J Comput Chem 14:1347–1363
32. Clark T, Alex A, Beck B, Chandrasekhar J, Gedeck P, Horn AHC, Hutter M, Martin B, Rauhut G, Sauer W, Schindler T, Steinke T (2005) VAMP 10.0. Computer-Chemie-Centrum. Universität Erlangen-Nürnberg, Erlangen
33. McIver JW (1974) The structure of transition states: are they symmetric? Jr Acc Chem Res 7:72–77. doi:10.1021/ar50075a002
34. Ermer O (1975) Determination of molecular symmetries by force field calculations and evaluation of symmetric and nonsymmetric conformational transition states avoiding complete point-by-point mapping. Tetrahedron 31:1849–1854. doi:10.1016/0040-4020(75)87040-2
35. Dionne P, St-Jacques M (1987) Mechanism of the gauche conformational effect in 3-halogenated 1,5-benzodioxepins. J Am Chem Soc 109:2616–2623. doi:10.1021/ja00243a012
36. Weinhold F (2003) Rebuttal to the bickelhaupt–baerends case for steric repulsion causing the staggered conformation of ethane. Angew Chem Int Ed 42:4188–4194. doi:10.1002/anie.200351777
37. Tapu DA, Dixon DA, Roe C (2009) 13C NMR spectroscopy of "Arduengo-type" carbenes and their derivatives. Chem Rev 109:3385–3407. doi:10.1021/cr800521g
38. Winget P, Horn AHC, Selçuki C, Martin B, Clark T (2003) AM1* parameters for phosphorus, sulfur and chlorine. J Mol Model 9:408–414
39. Winget P, Clark T (2005) AM1* parameters for aluminum, silicon, titanium and zirconium. J Mol Model 11:439–456
40. Kayi H, Clark T (2009) AM1* parameters for bromine and iodine. J Mol Model 15:295–308